Precipitation over Greenland and its relation to the North Atlantic Oscillation

David H. Bromwich,[1] Qiu-shi Chen, Yufang Li,[2] and Richard I. Cullather[3]

Polar Meteorology Group, Byrd Polar Research Center, Ohio State University, Columbus

Abstract. The ω equation method based on an equivalent isobaric geopotential height in σ coordinates has been used to retrieve the precipitation over Greenland. This approach is designed to accurately represent the topographic effects of the Greenland Ice Sheet on atmospheric motion and precipitation. The 11 year mean precipitation from 1985 to 1996 over all of Greenland is 376 mm yr^{-1}, which is close to the long-term mean precipitation of 346 mm yr^{-1} estimated from glaciological data. The precipitation over all of Greenland shows that the largest value in 1986 is 472 mm yr^{-1} and the smallest value in 1995 is 309 mm yr^{-1}. The major interannual variability of the atmospheric circulation in the North Atlantic can be represented by the variation of the North Atlantic Oscillation (NAO) index, which is most pronounced during winter. It is found that if the NAO index increases, the total precipitation over Greenland decreases, and vice versa. The correlation coefficient between these two series for 1985-1995 is -0.75. The mean precipitation over southern Greenland, where the majority of precipitation falls, is more closely related to the NAO index in winter, and their correlation coefficient is -0.80. This relationship can be understood from the composite maps of sea level pressure and Greenland precipitation for the high and low index months. During months of high NAO index values, the Icelandic Low is strong. During months of low NAO index values, the monthly mean low is located to the southwest of Greenland over the Labrador Sea. Precipitation amounts over the southeast coast of Greenland are about 100 mm larger during the low NAO index months than the high NAO index months. Precipitation over all of Greenland during the low NAO index months is higher. There are significant downward trends in annual precipitation from 1985-1995 for all of Greenland and its southern and central west coastal regions, amounting to about 3% per year.

1. Introduction

The major interannual variability of the atmospheric circulation in the North Atlantic region can be represented by the variation of the North Atlantic Oscillation (NAO) index. The NAO is a temporal fluctuation of the zonal wind strength across the North Atlantic Ocean due to pressure variations in both the subtropical anticyclone belt and the subpolar low near Iceland. An index of the NAO is the difference between normalized mean winter (December, January, and February) pressure anomalies at Ponta Delgada, Azores, and Akureyri, Iceland [*Rogers*, 1984]. (The winter sea level pressure (SLP) anomalies at each station are normalized by dividing the long-term standard deviation of the mean pressure.) The NAO is intimately related to the behavior of the Icelandic Low [Serreze et al., 1997].

Barlow et al. [1993, 1997], *White et al.*[1997], and *Rogers et al.* [1998] studied the marked connection between the NAO and the isotope variations in ice cores from near the Summit of Greenland. *Appenzeller et al.* [1998a] showed that the correlation coefficient between the ice accumulation (nearly equal to precipitation over most of the ice sheet) in western Greenland and NAO index is negative. Based on this correlation, *Appenzeller et al.* [1998b] used selected ice core data to reconstruct an annual proxy of the NAO index for the past 350 years, and then examined the long-term variability of the NAO using this annual proxy.

The variation of accumulation on the Greenland Ice Sheet cannot be understood without study of precipitation, especially its relation to the NAO index. Direct precipitation measurements for the whole ice sheet are impractical, and those in the coastal region have substantial uncertainty [*Bromwich and Robasky*, 1993] but are correctable with some effort [*Yang et al.,* 1999]. The analyzed wind, geopotential height, and moisture fields are available for recent years, and the precipitation is retrievable from these fields by an indirect dynamic approach.

In order to improve synoptic analyses and dynamic studies near high mountain regions, such as Greenland, an equivalent isobaric geopotential height, $\phi_e(x,y,\sigma,t)$, whose horizontal gradient is equal to the irrotational part of the horizontal pressure gradient force in σ coordinates, has been proposed

---

[1]Also at Atmospheric Sciences Program, Department of Geography, Ohio State University, Columbus, OH.
[2]Now at Department of Meteorology, Pennsylvania State University, University Park, PA.
[3]Now at Department of Aerospace Engineering Sciences, University of Colorado, Boulder, CO.

[Chen et al., 1997a; Chen and Bromwich, 1999]. This variable in σ coordinates plays the same role as the geopotential height $\phi(x,y,p,t)$ does in p coordinates, so it is referred to as the equivalent isobaric geopotential height in σ coordinates.

The 850 hPa and other lower levels over Greenland are actually below Earth's surface, and the vorticity and temperature advection cannot be meaningfully computed for these levels. Orographic effects are difficult to handle in the ω equation with p coordinates. Thus a generalized ω equation without the quasi-geostrophic approximation and based on the equivalent isobaric geopotential height in σ coordinates was developed by Chen and Bromwich [1999]; it was used to retrieve precipitation over Greenland for 1987 and 1988 [Chen et al., 1997a], with reasonable results being obtained. The relationship between precipitation and cyclonic activity near Greenland was also studied.

In this paper, this ω equation method is further used to retrieve the precipitation over Greenland for 11 years from 1985-1995 based on the twice daily operational analyses at 0000 and 1200 UTC from the European Centre for Medium-Range Weather Forecasts (ECMWF). The seasonal and interannual variations of the precipitation for these 11 years over Greenland and its sub regions are evaluated. Because the spatial resolution of the variations of Greenland precipitation retrieved by this dynamic method is higher than those computed from other methods [Bromwich et al., 1998], the relationship between the NAO index and precipitation over Greenland and its sub regions can be studied in some detail.

It is shown by Chen et al. [1997a] that the most important weather system producing precipitation over Greenland is the frontal cyclone. The position and intensity of the monthly mean cyclone near the Greenland area have a close relationship to the precipitation over that region. The NAO is also intimately related to the features of the mean Icelandic Low. Thus the physical basis of the relationship between precipitation over Greenland and the NAO is discussed.

2. Precipitation Over Greenland and Its Seasonal and Interannual Variations

2.1. Retrieved Mean Precipitation Over Greenland for 1985-1995

The generalized ω equation without the quasi-geostrophic approximation and based on the equivalent isobaric geopotential height in σ coordinates is shown by Chen et al. [1997a] and Chen and Bromwich [1999]. The procedure for computing precipitation from the vertical motion is presented in the appendix. The precipitation is calculated twice per day based on the operational analyses at 0000 and 1200 UTC from ECMWF. The annual precipitation is derived by adding daily precipitation amounts for 1 year.

Four-dimensional data assimilation (FDDA) systems for limited regions are still under development and are computationally very demanding. Because we only want to determine the primary features of the annual precipitation over Greenland, the simple dynamic method is adequate for our application.

The computational domain and topography of Greenland are presented in Figure 2b of Chen et al. [1997a]; the mesh size is 111x81, and grid spacing is 50 km. Using this ω equation method, the mean annual precipitation distribution

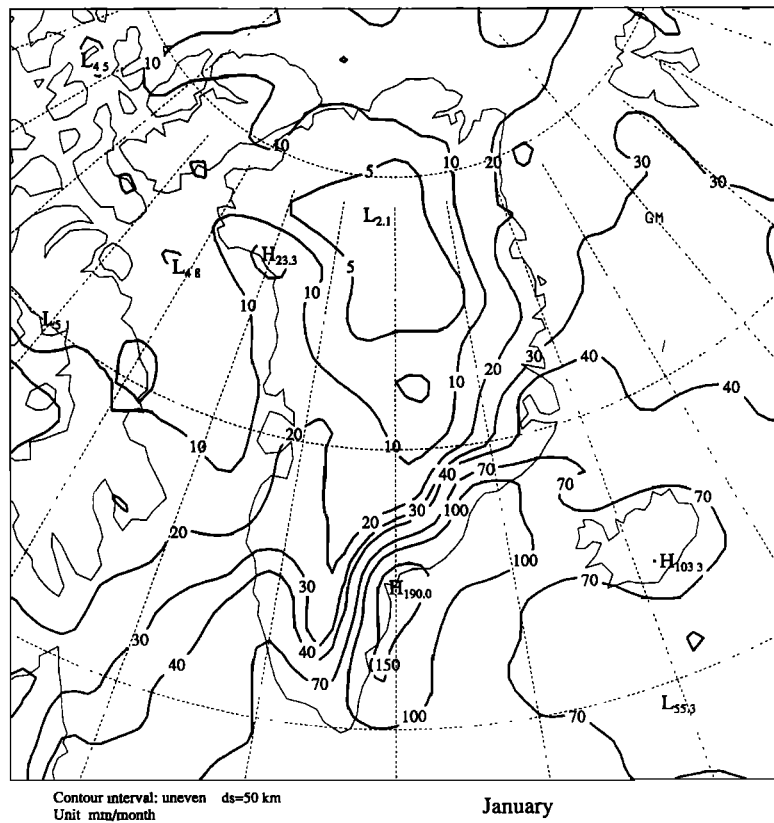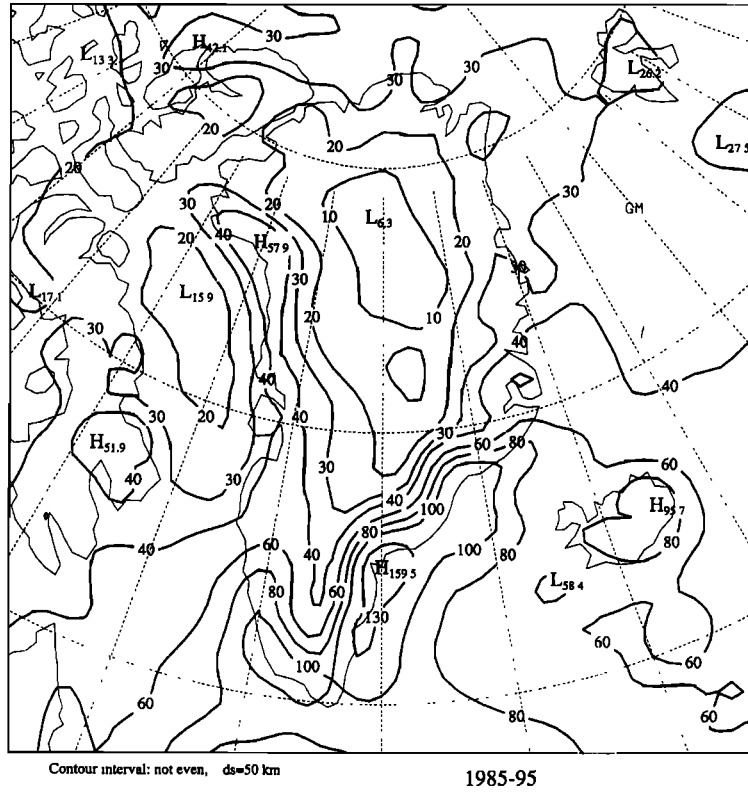for 11 years from 1985 to 1995 has been calculated and is shown in Figure 1a.

The spatial distribution of the long-term accumulation synthesized from glaciological data is described by Ohmura and Reeh [1991], Ohmura et al. [1999], and Bromwich et al. [1998]. The last authors also examined several atmospherically derived precipitation estimates over Greenland in comparison to glaciological data and to each other. These precipitation estimates include the average spatial distribution of precipitation minus evaporation or sublimation (P-E) derived from the atmospheric moisture budget using ECMWF operational analyses, the ECMWF Reanalysis (ERA) forecast precipitation [Gibson et al., 1996], the National Centers for Environmental Prediction / National Center for Atmospheric Research (NCEP/NCAR) reanalysis forecast precipitation [Kalnay et al., 1996], the precipitation diagnosed from the Keen model [Bromwich et al., 1993] and the precipitation retrieved by the ω equation method [Chen et al., 1997a; Chen and Bromwich, 1999]. From the comparison, it is concluded that there is general agreement on a long-term Greenland average of about 350 mm yr^{-1}, but none of the precipitation estimates is able to capture all of the regional-scale features. It is also found that the ω equation method appears to be most useful for obtaining a high-resolution depiction of precipitation over Greenland [Bromwich et al., 1998].

2.2. Seasonal Variation of Monthly Mean Precipitation Over Greenland and Its Sub Regions

In order to show precipitation in different seasons, the mean precipitation distributions in January and July averaged for 1985-1995 are shown in Figures 1b and 1c, respectively. It is seen that precipitation over the southern part of Greenland along the southeastern and southwestern coasts is larger in January (winter) than in July (summer). However, the precipitation over the northern part, including its western and northern coasts and central interior region, is larger in July (summer) than in January (winter). The seasonal precipitation variations measured at coastal stations agree with this depiction [Berthelsen et al., 1993, p. 32]. The seasonal variations of precipitation over the southern and northern parts of Greenland are opposite, and greater precipitation amounts in these two parts occur in January and July, respectively. Thus it is advantageous to separate Greenland into several sub regions to study their seasonal features. Greenland has been divided by Chen et al. [1997a] into five sub regions, which are referred to as the northern coastal region, central-east and central-west coastal regions, central interior region, and southern region, as shown in Figure 2.

The annual cycles of monthly mean precipitation values averaged for 1985-1995 over the northern coastal region and central interior region are shown in Figure 3a. This figure shows that the largest precipitation over the northern region occurs in July and the smallest in January. The seasonal variability of precipitation over the central interior region is similar.

The variations of the monthly mean precipitation for the southern region of Greenland are presented in Figure 3b. The smallest monthly mean precipitation occurs in July, but there are several maxima, for example, February and November. The mean precipitation is larger than 600 mm yr^{-1} for all months in this region except July.

Contour interval: not even,   ds=50 km   1985-95

Contour interval: uneven   ds=50 km
Unit mm/month   January

Figure 1. (a) The retrieved annual mean precipitation for 1985-1995 in centimeters with a contour interval of 20 cm, but 10 cm if smaller than 40, and 30 cm if larger than 100. (b) The computed monthly mean precipitation for January from 1985-1995 in mm with a contour interval of 30 millimeters, but 50 mm if larger than 100 mm, 10 mm if less than 40 mm, and 5 mm if less than 10 mm. (c) Same as Figure 1b but for July.
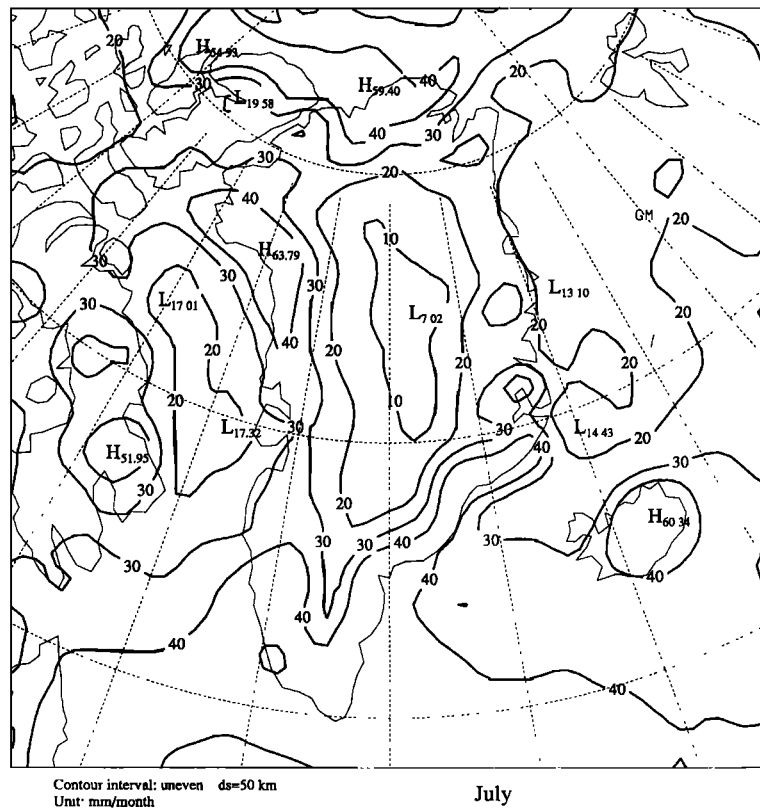
Contour interval: uneven   ds=50 km
Unit: mm/month   July

Figure 1. (continued)

The annual cycle of the monthly mean precipitation averaged for the 11 years over the central-west coastal region is presented in Figure 3c. The variation of the mean values is similar to Figure 3a. Precipitation is lower in winter and higher between May and November, with the largest value occurring in August. The corresponding monthly mean precipitation values for the central-east coastal region are also

Figure 2. The separation of Greenland into major regions (solid lines) and subregions (dashed lines). S, the southern region; N, the northern coastal region; C-W, the central west coastal region; C, the central interior region and C-E, the central east coastal region.

shown in Figure 3c. The seasonal precipitation variation in this region is not well defined.

The annual variation of the monthly mean precipitation for all of Greenland averaged over the 11 years and the associated standard errors are presented in Figure 3b. Because the majority of Greenland precipitation falls in the southern region, the maximum months (February, May, and November) of the two curves in Figure 3b are the same, but the amplitude of annual variation over all of Greenland is much smaller than that over the southern region. The standard errors of the mean values for all of Greenland are very small. Because the seasonal variations of precipitation over the southern region are opposite to those over the northern coastal, central-west coastal, and central interior regions, the average seasonal variation for the combination of these two kinds of region must be relatively small.
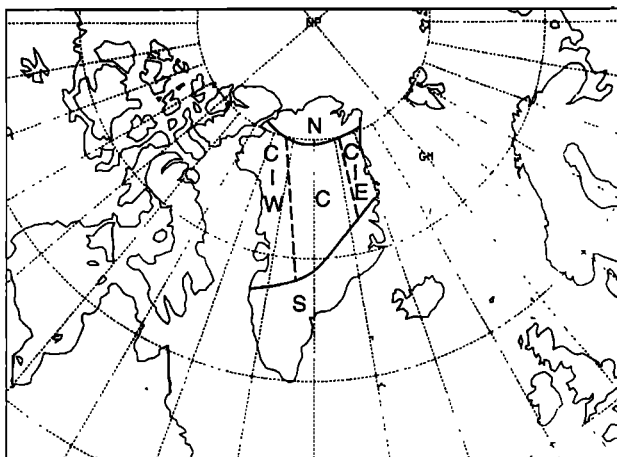
2.3. Interannual Variations of Precipitation Over Greenland and Its Sub Regions

The interannual variation of the mean precipitation over all of Greenland from 1985 to 1995 is shown in Figure 4a. The largest amount (472 mm yr^{-1})occurs in 1986, and the smallest amount (309 mm yr^{-1}) occurs in 1995. The 11 year mean precipitation over all of Greenland is 376 mm yr^{-1}, and the standard deviation is 41 mm yr^{-1}.

The annual mean precipitation for all of Greenland, estimated from glaciological data over the ice sheet and meteorological observations in the coastal areas, is about 340 mm yr^{-1} [*Ohmura and Reeh*, 1991]. Recently, *Ohmura et al.* [1999] derived a more accurate estimate of 346 mm yr^{-1}. Using numerical simulations, *Ohmura et al.* [1996] found that
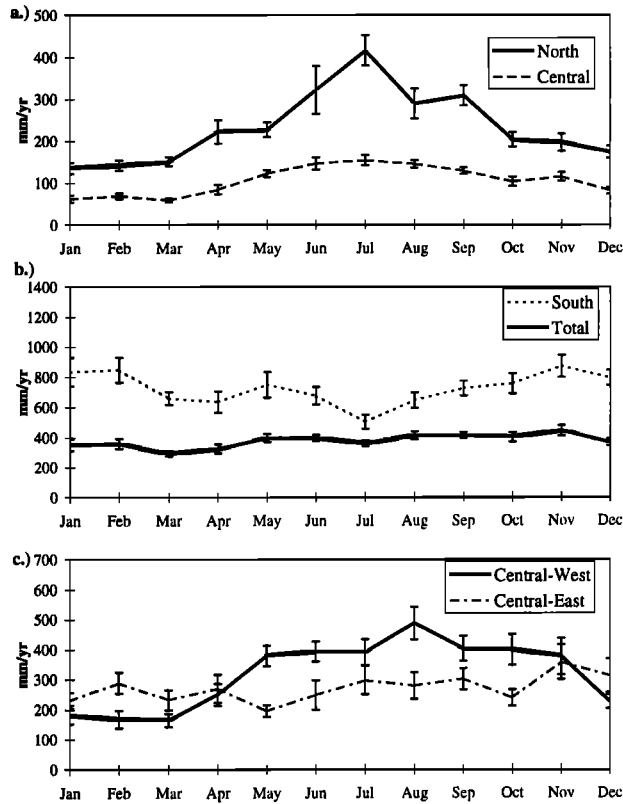
Figure 3. (a) The mean monthly precipitation averaged for 1985-1995 over the north coastal and central interior regions (with ±1 standard error shown by the vertical bars associated with each mean value). (b) Same as Figure 3a but over the southern region and all of Greenland (called total) except that the scale for precipitation is amplified. (c) Same as Figure 3a but over the central-west coastal and central-east coastal regions.

a global climate model with horizontal resolutions of T21, T42, and T106 produced mean precipitation amounts of 785, 585, and 494 mm yr^{-1} for all of Greenland, respectively. As the resolution increased, the overestimation of precipitation decreased. The mean value 376 mm yr^{-1} is closer to 346 mm yr^{-1} than 494 mm yr^{-1}, which is simulated by the ECHAM3/T106 model for 5 1/2 years [*Ohmura et al.*, 1996].

The interannual variation over the southern region of Greenland for the 11 years is also shown in Figure 4a. Because the majority of precipitation over Greenland falls over the southern region, the variation pattern for the southern region is similar to that for all of Greenland. The largest mean precipitation in 1986 is 870 mm yr^{-1}, and its smallest value in 1995 is 530 mm yr^{-1}. The 11 year mean value for precipitation over southern Greenland is 723 mm yr^{-1}, and the standard deviation is 106 mm yr^{-1}. Thus the interannual variability of precipitation over the southern region is larger than that over all of Greenland.

The interannual variations of the mean precipitation over the other regions of Greenland are generally different. Those over the northern coastal, central-west, central interior, and central-east regions for the 11 years are shown in Figure 4b. It is seen that the interannual variability of precipitation over the central interior region of Greenland is very small, while the

variability for the central-west resembles that for all of Greenland.

3. Interannual Variation of Precipitation Over Greenland and Its Relation to the NAO in Winter

3.1. Relationships Between the NAO Index and Precipitation Over Greenland and Its Sub Regions

The correlation coefficients between the NAO index and the precipitation over various subregions and all of Greenland, and for four seasons (winter (DJF), spring (MAM), summer (JJA), and fall (SON)) and all of the year are shown in Table 1. The total precipitation for winter 1986 (for example) denotes the sum of the precipitation for December 1985 and January and February 1986. The slightly modified monthly NAO index of *Hurrell* [1995], which contrasts the pressures at Lisbon with those at Stykkishholmur, Iceland, is used here, and the values are averaged for each season. Figure 5a shows the interannual variations of the total precipitation over all of Greenland and the NAO index in winter. It is seen from Figure 5a that if the NAO index (which is shown inverted on the right side of the figure) in winter increases, the total precipitation in winter over Greenland decreases. The correlation coefficient between them in winter is -0.75. Thus the interannual variations of the mean precipitation over all of Greenland have a close relation to those of the NAO index in winter.

The majority of precipitation over Greenland falls over the southern region. The interannual variations of the mean precipitation over southern Greenland and NAO index in winter are shown in Figure 5b. The correlation coefficient between these two series in winter shown in Table 1 is -0.80, and the absolute value of this coefficient is slightly larger than that between the mean precipitation over all of Greenland and the NAO index.

The interannual variations for the precipitation over the central west coastal region and those of the NAO index in winter and fall are shown in Figures 5c and 5d, respectively. The corresponding correlation coefficients are also relatively large at -0.65 and -0.60, respectively. All of the above correlation coefficients are statistically significant at better than the 92% confidence level using a one-sided t-test [*Haan*, 1977] and accounting for the impact of autocorrelation by the method of *Angell* [1981].

Recently *Appenzeller et al.* [1998a] showed the negative correlation coefficient between the ice accumulation and NAO index is stronger in west central Greenland. However, it should be pointed out that the correlation coefficients between

Table 1. Correlation Coefficients Between Precipitation Amount and the NAO index for 1985-1995

Region	DJF	MAM	JJA	SON	Annual
North	-0.24	0.21	0.10	-0.02	0.36
Central-west	-0.65	0.24	0.05	-0.60	0.00
Central	-0.39	0.14	0.24	0.06	0.55
Central-east	0.05	0.09	0.14	0.57	0.64
South	-0.80	0.09	0.10	-0.16	-0.02
Greenland	-0.75	0.17	0.15	-0.24	0.13
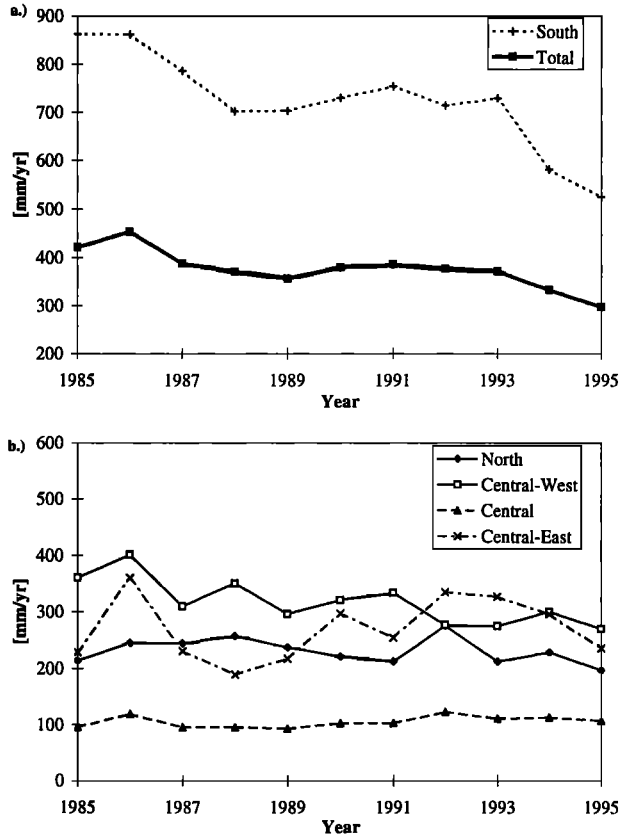
Figure 4. The variations for 1985-1995 of the annual mean precipitation averaged over (a) the southern region and all of Greenland and (b) the north coastal, central interior, central-west coastal, and central-east coastal regions.

the precipitation over the central west coastal region and the NAO index are relatively large only for winter and fall but not for all of the year. Our results also show that the absolute value of the correlation coefficient in southern Greenland is the largest in winter.

3.2. Physical Basis and Composite Maps for the Relationship Between the NAO and Greenland Precipitation in Winter

Because the NAO is intimately related to the behavior of the Icelandic Low [*Serreze et al.* 1997], the above correlation can easily be understood from the cyclonic activity near Greenland. It was shown by *Chen et al.* [1997a] that if the monthly mean low is located near Iceland, precipitation over Greenland during that month will be reduced. By contrast, if the monthly mean low is centered in the Labrador Sea, enhanced precipitation will fall over Greenland. Thus the position and intensity of the monthly mean cyclone have a close relationship to the precipitation over Greenland. Precipitation variations in the southern region of Greenland are more closely related to the position and intensity of the Icelandic Low. This is the reason why the absolute value of the correlation coefficient is larger in this region than in the others.

In order to give a clear picture of the relationship between

the NAO and Greenland precipitation, composite precipitation maps for the high and low values of the monthly NAO index are shown in Figures 6a and 6b, respectively. Among the 33 winter months (DJF) of 1985-1995, it is found that the NAO index values for 9 months (01/86, 12/86, 01/89, 02/89, 02/92, 01/93, 12/93, 01/95, and 02/95, where 01/86 is January 1986, for example) are greater than +1.7 and those for 5 months (01/85, 02/85, 02/86, 01/87, and 12/89) are less than -1.4. Figures 6a and 6b are produced by averaging the monthly precipitation over the nine high NAO index months and the five low NAO index months, respectively. Figures 6c and 6d are the corresponding composite sea level pressure (SLP) maps for the high and low NAO index months.

From Figure 6c, it is easily seen that during the months of the high NAO index values, the Icelandic Low is strong. During the months of the low NAO index values (Figure 6d), the monthly mean low is located to the southwest of Greenland over the Labrador Sea. Comparing Figure 6a with 6b, precipitation amounts in the southeast coast of Greenland during the low NAO index months are about 100 mm larger
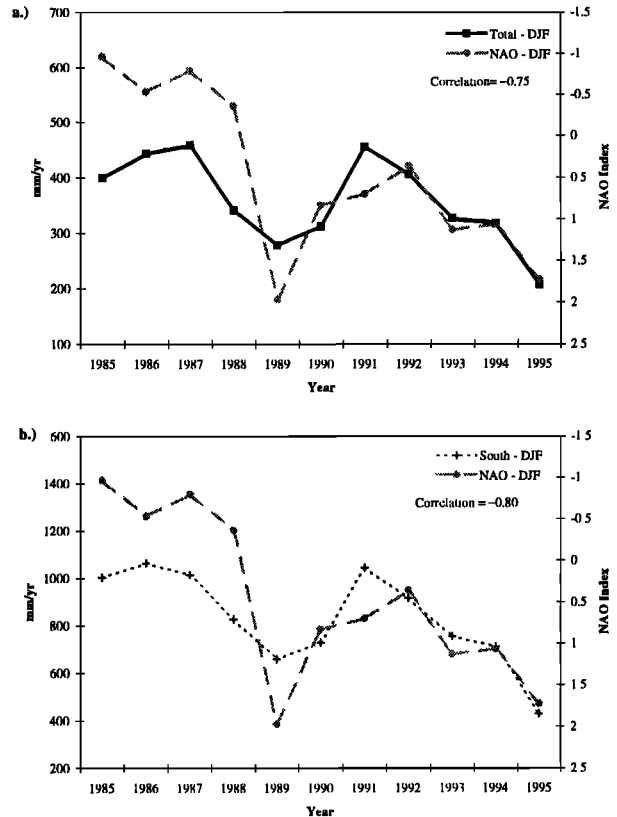
Figure 5. (a) The interannual variations for the mean values in winter (DJF) of precipitation averaged over all of Greenland (heavy solid line) and those of the NAO index (dashed line). Note that the NAO index scale is inverted. (b) Same as Figure 5a but for the precipitation averaged over the southern region of Greenland (thin dashed line). (c) Same as Figure 5b but for the precipitation averaged over the central-west coastal region (heavy solid line) in winter (DJF). (d) Same as Figure 5b but for the mean precipitation over the central-west coast region (heavy solid line) in fall (SON).
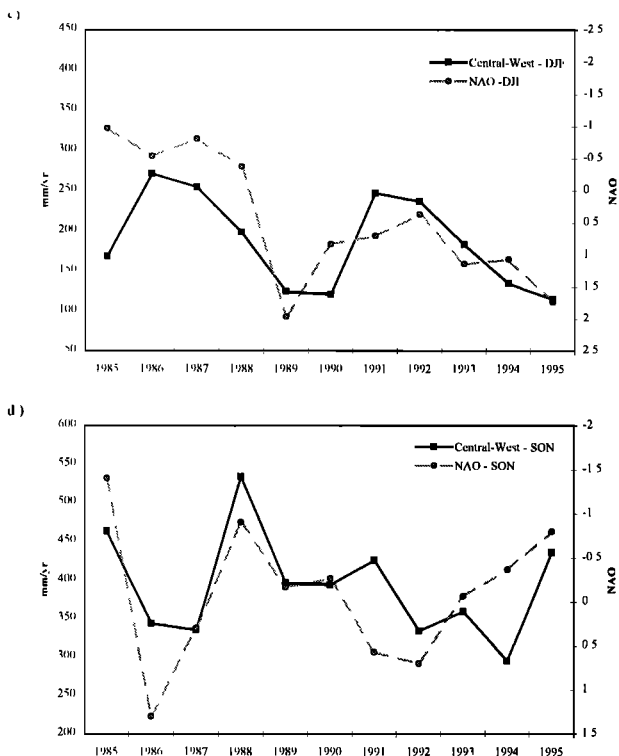
Figure 5. (continued)

than the high NAO index months. Precipitation over all of Greenland during the low NAO index months is higher. These analyses are in agreement with the relationship between Greenland precipitation and cyclonic activity studied by *Chen ct al.* [1997a]

The NAO index is calculated from the SLP readings at two stations. Relating Greenland precipitation to the NAO station index in seasons other than winter may not be physically meaningful because the dominant spatial pattern of atmospheric circulation variability (for example, the leading empirical orthogonal function of sea level pressure) over the Atlantic-Arctic sector does not necessarily coincide with the two-station index used for the NAO [*Hurrell and van Loon*, 1997]. Thus Table 1 shows that the correlation coefficients for spring (MAM) and summer (JJA) are very small, which means that there is little relation between Greenland precipitation and the NAO two-station index. The NAO index may not be representative of the cyclonic activity near Greenland in MAM and JJA.

3.3. Relationship Between the Precipitation and Temperature Over Greenland in Winter

It is known that the monthly mean temperature anomaly over Greenland is intimately related to the NAO, which is expressed by a seesaw in mean winter temperatures between Greenland and northern Europe [*van Loon and Rogers*, 1978; *Rogers and van Loon*, 1979; *Meehl and van Loon*, 1979]. The occurrences of the seesaw were directly determined by using temperatures at Oslo, Norway, and Jakobshavn, Greenland. One phase of NAO is called "Greenland above" when Jakobshavn temperatures are above normal (Oslo below

normal); the other phase is called "Greenland below" in which Jakobshavn temperatures are below normal (Oslo above normal). "Greenland above" occurs when the NAO index is low, while "Greenland below" occurs during the high NAO index values.
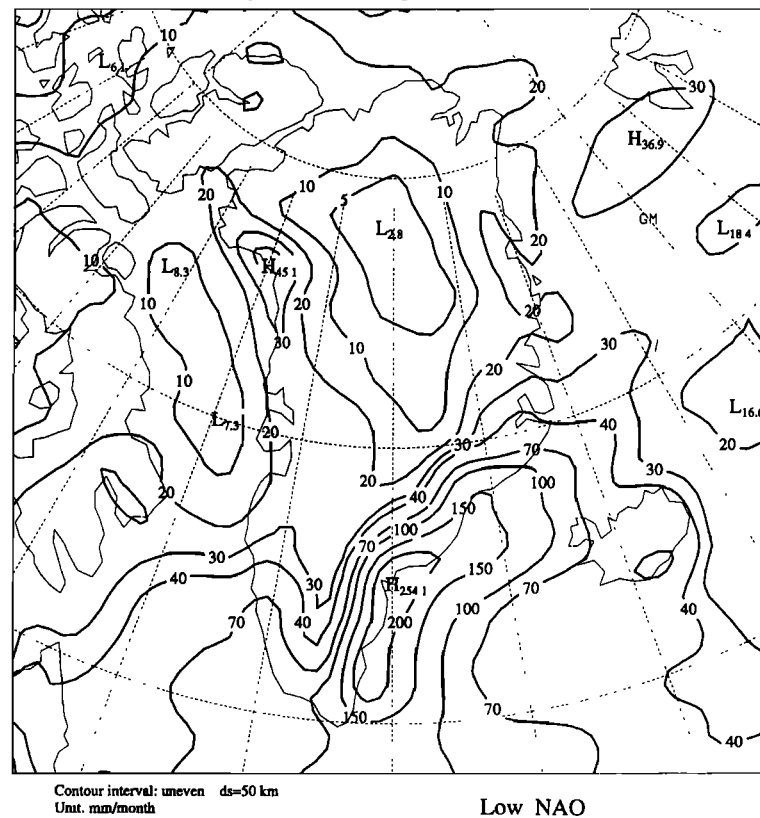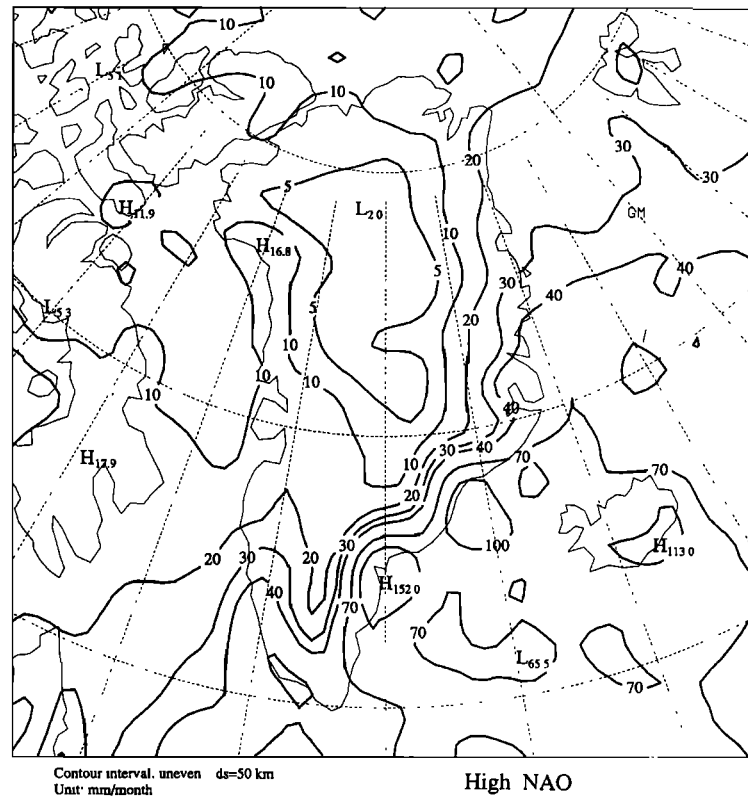
Because the "Greenland above" and "Greenland below" are based on the winter temperature in Greenland, the relationship between the precipitation and temperature in winter has been examined. The temperatures given by the ECMWF operational analyses are averaged for all of Greenland at 2 m above the surface and at the 500 hPa level. The interannual variations of the mean temperature in winter (DJF) over all of Greenland for these two levels are shown in Figure 7a. It is seen that if the mean temperature decreases, the mean precipitation over all of Greenland also decreases, and vice versa. The correlation coefficients of the mean temperatures at 2 m above the ground and at 500 hPa level with the mean precipitation are 0.64 and 0.69, respectively. Thus the "Greenland above" and "Greenland below" are associated not only with higher and lower mean temperature but also with higher and lower mean precipitation over Greenland in winter, respectively. The correlation coefficients of the mean temperatures at 2 m above the ground and at the 500 hPa level with the NAO index in winter are -0.77 and -0.85, respectively.

The "Greenland above" and "Greenland below" in temperature can also easily be understood from the composite mean SLP maps in Figures 6c and 6d. The "Greenland below" pattern corresponds to Figure 6c, which shows that the Atlantic westerlies are anomalously strong and the Iceland Low is also strong with Oslo and Jakobshavn located to its east and west, respectively. The temperature at Oslo above normal is due to the warm air advection from the southwesterly warm flow and that at Jakobshavn below normal is due to the northerly cold air flow. During the "Greenland above," the mean low is located to the southwest of Greenland as shown in Figure 6d. The relatively high temperatures in Greenland are due to prevalent southeasterly warm flow over the southern part of Greenland. Thus the temperature anomalies in the Greenland region during the different phases of the NAO are caused by differences in warm and cold air advection associated with the mean large-scale circulation.
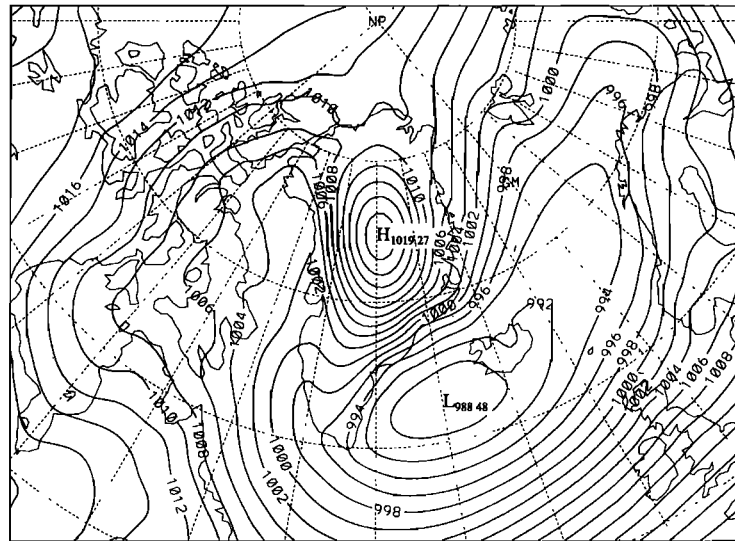
3.4. Downward Trend in Annual Precipitation Over Greenland From 1985-1995

There is a downward trend in annual precipitation from 1985-1995 for all of Greenland and its southern region. The downward trends based on linear regression equations for all of Greenland and for the southern region are shown in Figure 7b and are about -10 ± 2 mm yr^{-1} or 2.7% per year, and -26 ± 5 mm yr^{-1} or 3.7% per year, respectively. There is also a downward trend for the central west region (Figure 4b) of about -10 ± 3 mm yr^{-1} or 2.4% per year.

Bromwich et al. [1998] noted that, among the five evaluated approaches, the ω equation method was the only one which produced decreasing annual precipitation amounts for southern Greenland. The annual accumulation values for the same period (1985-1995) from three ice core sites in southern Greenland confirm this downward precipitation trend (*J McConnell et al.*, Annual Snow Accumulation on the Greenland Ice Sheet (1985-1996): New Observations versus

Contour interval. uneven   ds=50 km
Unit· mm/month   **High NAO**

Contour interval: uneven   ds=50 km
Unit. mm/month   **Low NAO**

Figure 6. (a) The composite monthly precipitation maps for the high NAO index months (in millimeters with a contour interval of 30 mm, but 50 mm if larger than 100 mm, 10 mm if less than 40 mm, and 5 mm if less than 10 mm). (b) Same as Figure 6a but for the low NAO index months. (c) The composite sea level pressure maps for the high NAO index months (in hPa with the contour interval of 2 hPa). (d) Same as Figure 6c but for the low NAO index months.

High NAO

Contour interval: 2 mb   ds=50 km
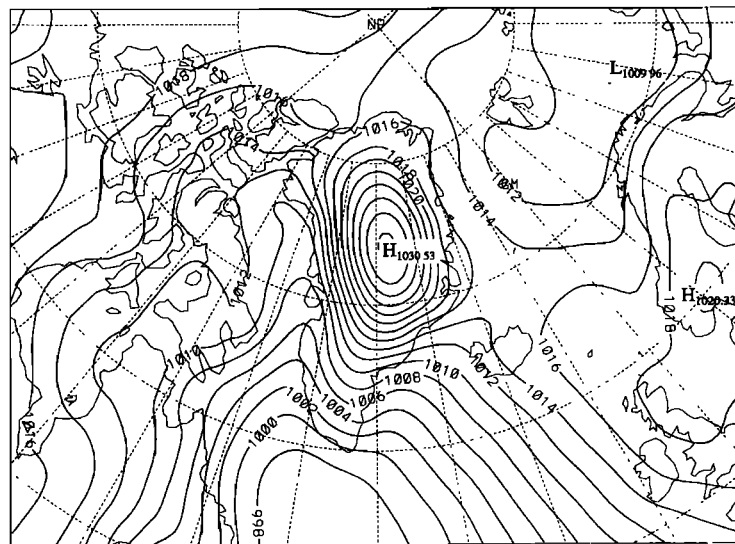
Low NAO

Contour interval: 2 mb   ds=50 km

Figure 6. (continued).

Model Predictions, submitted to Journal of Geophysical Research, 1999).

This downward trend in precipitation during 1985-1995 is consistent with other studies. *Chapman and Walsh* [1993] have also found that, in contrast to all other areas of the Northern Hemisphere north of 50°N, southern Greenland and the adjacent waters of Baffin Bay, the Labrador Sea, and North Atlantic have undergone a significant cooling in the surface air temperature over the period 1960-1990. This cooling ranges between 0.25° to 0.5°C per decade over this region and is manifested in all seasons, although most striking in autumn and winter. They also reported changes in Arctic sea ice extent over the last three decades, and found ice extents increasing over Baffin Bay and the Labrador Sea.

Bromwich et al. [1993] found that the striking feature of the total precipitation change over all of Greenland for the period 1963-1988 is a downward trend amounting to about 15-20% over the 26 years; this finding was supported by *Bromwich et al.* [1998]. The downward trend in precipitation during 1985-1995 shown in Figure 6 continues the downward trend after the period 1963-1988.

Hurrell [1995] found that there are long-term variations in the NAO index. Since the early 1970s the NAO index exhibited an upward trend. In the 1980s, NAO index values became unprecedentedly positive. Over the past decade, the NAO has contributed significantly to the recent winter
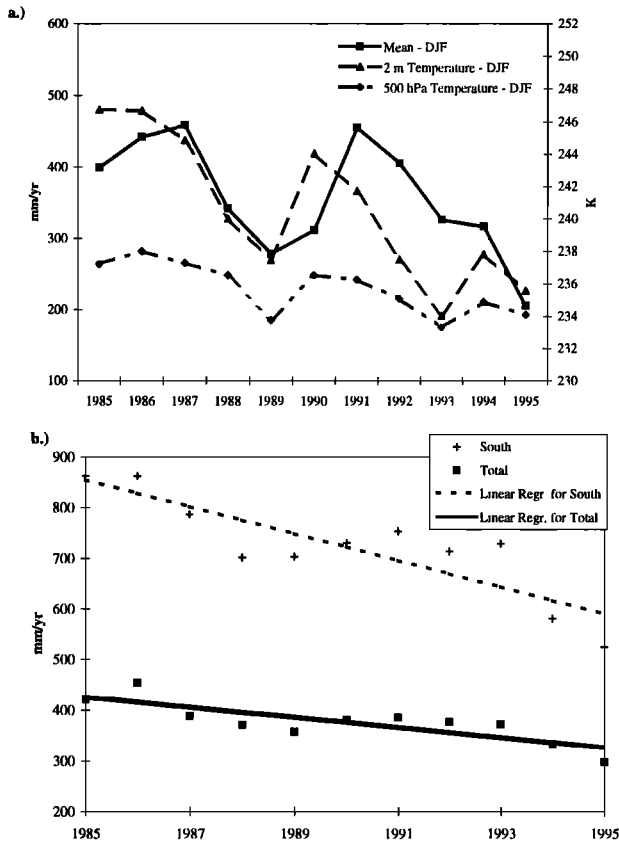
Figure 7. (a) The interannual variations in winter (DJF) for the mean precipitation over all of Greenland (heavy line), for the temperature at 2 m above the surface of the ice sheet (dashed line) and for the temperature at the 500 hPa level over the ice sheet (long and short dashed line). (b) A downward trend of the annual mean precipitation from 1985-1995 shown by linear regression for the southern region and all of Greenland.

warmth across Europe and to the cold conditions in the northwest Atlantic. The long-term variations in the NAO index may also contribute to the downward trend in annual precipitation over Greenland during the last 30 years.

4. Conclusions

The ω equation method based on an equivalent isobaric geopotential height σ coordinates has been used to retrieve the precipitation over Greenland for 11 years from 1985 to 1995. This method has a better capability to deal with topographic effects than models without the equivalent geopotential. The 11 year mean value is 376 mm yr^{-1} and the standard deviation is 41 mm yr^{-1}. The largest value in 1986 is 472 mm yr^{-1}, and the smallest value in 1995 is 309mm yr^{-1}. The mean precipitation over all of Greenland from the glaciological data is about 346 mm yr^{-1} [*Ohmura et al.*, 1999]. The mean value 376 mm yr^{-1} for the 11 years is closer to 346 mm yr^{-1} than the 494 mm yr^{-1} simulated with the ECHAM3/T106 model for 5 1/2 years [*Ohmura et al.*, 1996].

The variation of the NAO is most pronounced during winter. The relationship between the mean precipitation over Greenland and NAO index in winter has been examined. The correlation coefficient between these two series for 1985-1995 is -0.75, and it is shown that if the NAO index increases,

the mean total precipitation over Greenland decreases. The mean precipitation over southern Greenland, where the majority of Greenland precipitation falls, is more closely related to the NAO index in winter. The correlation coefficient between them for 1985-1995 is -0.80. This result differs from that of *Appenzeller et al.* [1998a], who showed that the negative correlation coefficient between the ice accumulation and NAO index is stronger for west central Greenland.

The relationship between the precipitation over Greenland and NAO index can be understood from the composite maps of SLP and Greenland precipitation for the high and low NAO index months. During the months of the high NAO index values, the Icelandic Low is strong. During the months of the low NAO index values, the monthly mean low is located to the southwest of Greenland over the Labrador Sea. Precipitation amounts in the southeast coast of Greenland during the low NAO index months are about 100 mm larger than the high NAO index months. Precipitation over all of Greenland during the low NAO index months is higher.

The correlation coefficients of the mean temperatures at 2 m above the ground and at the 500 hPa level with the mean precipitation in winter over all of Greenland are 0.64 and 0.69, respectively. The "Greenland above" and "Greenland below" patterns are associated not only with higher and lower mean temperature but also with higher and lower mean precipitation in winter over Greenland, respectively.

There are also significant downward trends in annual precipitation from 1985-1995 (about 3% per year) for all of Greenland and for its southern and central west coastal regions.

Appendix: Brief Description for the Precipitation Retrieval Method Based on a Generalized ω Equation With the Equivalent Geopotential in σ Coordinates

A1. Equivalent Geopotential in σ Coordinates

The horizontal wind can be separated into its irrotational and rotational parts and expressed by

$$\vec{V} = -\nabla\chi - \vec{k} \times \nabla\psi, \tag{A1}$$

where χ and ψ denote velocity potential and stream function, respectively. The horizontal pressure gradient force $\bar{G}$ in σ coordinates is expressed by

$$\vec{G} = -\nabla\phi(x,y,\sigma,t) - RT\nabla\ln p_*(x,y,t), \tag{A2}$$

where $\phi(x,y,\sigma,t)$ and $p_*(x,y,t)$ are the geopotential and surface pressure, respectively. Here $\bar{G}$ is also a horizontal vector, and it can also be separated into its irrotational and rotational components and expressed by

$$\vec{G} = -\nabla\phi_e - \vec{k} \times \nabla\eta, \tag{A3}$$

where $\phi_e(x,y,\sigma,t)$ is referred to as an equivalent geopotential, $\eta(x,y,p,t)$ is called a geo-streamfunction [*Chen and Bromwich*, 1999].

Because the horizontal pressure gradient force $-\nabla\phi(x,y,p,t)$ in P coordinates is also irrotational, the equivalent geopotential $\phi_e(x,y,\sigma,t)$ can be used in σ coordinates in the same way as $\phi(x,y,p,t)$ is used in P

coordinates. The equivalent geopotential ϕ_e can be used in synoptic analysis on constant σ surface.

The irrotational part $-\nabla\phi_e(x,y,\sigma,t)$ must be equal to the irrotational part of the total vector on the right-hand side of (A2). Thus we have

$$\nabla^2\phi_e(x,y,\sigma,t) = \nabla^2\phi(x,y,\sigma,t) + \frac{\partial}{\partial x}\left(RT(x,y,\sigma,t)\frac{\partial\ln p_*}{\partial x}\right)$$
$$+ \frac{\partial}{\partial y}\left(RT(x,y,\sigma,t)\frac{\partial\ln p_*}{\partial y}\right).$$

(A4)

If equation (A4) is solved in a limited region, the equivalent isobaric geopotential in σ coordinates can be separated into its inner and harmonic parts [*Chen and Kuo*, 1992] as

$$\phi_e = \phi_{eh}(x,y,\sigma,t) + \phi_{ei}(x,y,\sigma,t).$$

(A5)

Based on (A4), the inner part of the equivalent isobaric geopotential height in σ coordinates, ϕ_{ei}, can be derived from the solution of the following Poisson equation

$$\nabla^2\phi_{ei} = \nabla^2\phi_i + \frac{\partial}{\partial x}\left(RT\frac{\partial\ln p_*}{\partial x}\right) + \frac{\partial}{\partial y}\left(RT\frac{\partial\ln p_*}{\partial y}\right),$$

(A6)

with zero Dirichlet boundary value.

The equivalent geopotential in σ coordinates can be utilized to improve synoptic analysis [*Chen and Bromwich*, 1999] and numerical model predictions over high mountain regions. Some small but strong high pressure systems in the SLP analysis often occur over Greenland due to pressure reduction to the sea level. These artificial systems can be removed by equivalent geopotential analysis at σ=0.995. The geostrophic wind relation between the equivalent isobaric geopotential and stream function at σ=0.995 is approximately satisfied near high mountain regions. Thus the geostrophic wind relation for synoptic-scale motions is approximately satisfied directly on the constant σ surface between the equivalent geopotential and wind.

A2. Generalized ω Equation in σ Coordinates and a Simple Method for Computing Precipitation

The equivalent isobaric geopotential can be used to develop a generalized ω equation without the quasi-geostrophic approximation in σ coordinates to improve ω calculation over Greenland. The vertical coordinate σ is defined by σ=p/p* where p*(x,y,t)is the surface pressure. In the vertical, 16 σ levels at σ=0.025, 0.075, 0.125, 0.170, 0.240, 0.325, 0.430, 0.550, 0.610, 0.670, 0.775, 0.855, 0.915, 0.955, 0.980, and 0.995 are used. A variable X↓ is a column vector denoted by

$$X\!\downarrow=(X_1 \ldots, X_k, \ldots, X_N)^T,$$

(A7)

where (...)^T is for transpose. Using the continuity equation and vertical finite differencing, the pressure vertical velocity in σ coordinates can be expressed by

$$\left(\frac{\omega}{p}\right)\!\downarrow = m^2(I - C)\left(U\!\downarrow\frac{\partial\ln p_*}{\partial x} + V\!\downarrow\frac{\partial\ln p_*}{\partial y}\right) - m^2CD\!\downarrow,$$

(A8)

where C is a lower-triangular matrix [*Chen et al.* 1997b].

The Coriolis parameter and map scale factor are separated into

$$f = f_o + f', \qquad m^2 = \left(m^2\right)_o + \left(m^2\right)', \qquad \text{(A9)}$$

where f_o and $(m^2)_o$ are the average values in the integration region and f' and (m2)' are their deviations. The inner part of the equivalent isobaric geopotential can be separated into geostrophic and ageostrophic parts. The geostrophic part is expressed by $\phi_{eig} = f_o\psi_i$, while the ageostrophic part is denoted by

$$\phi_{eia} = \phi_{ei} - \phi_{eig} = \phi_{ei} - f_o\psi_i.$$

(A10)

If the atmospheric motion is quasi-geostrophic, the ageostrophic geopotential always vanishes.

The vorticity and divergence equations can be transformed into the equations of the inner parts of the stream function and velocity potential, respectively, and they are expressed by

$$\frac{\partial\psi_i}{\partial t}\!\downarrow + f_o\chi_i\!\downarrow = \psi_{adv,i}\!\downarrow$$

(A11)

$$\frac{\partial\chi_i}{\partial t}\!\downarrow + \phi_{eia}\!\downarrow = \chi_{adv,i}\!\downarrow - E_i\!\downarrow,$$

(A12)

where $E_i\!\downarrow=[m2(U2+V2)_i/2]\!\downarrow$, and the terms $\psi_{adv,i}\!\downarrow$ and $\chi_{adv,i}\!\downarrow$ are the variation rates of the inner parts of the stream function and velocity potential caused by advection, respectively. The equation of the ageostrophic geopotential can be written as

$$\frac{\partial\phi_{eia}}{\partial t}\!\downarrow + m_o^2A\nabla^2\chi_i\!\downarrow - f_o^2\chi_i\!\downarrow = \Phi_{e,had,ia}\!\downarrow + m_o^2AD_h\!\downarrow,$$

(A13)

where $\Phi_{e,had,ia}\!\downarrow$ is referred to as the variation rate of the ageostrophic geopotential caused by advection and diabatic heating, and A is a matrix [*Chen et al.* 1997b]. Here

$$D_h\!\downarrow=D\!\downarrow-D_i\!\downarrow,$$

(A14)

where D_i and D_h are the inner and harmonic parts of divergence, respectively [*Chen and Kuo*, 1992].

If the tendencies of the velocity potential and ageostrophic geopotential in (A12) and (A13) are neglected, this approximation is referred to as a balanced ageostrophic approximation [*Chen et al.* 1996]. Thus equation (A13) becomes

$$m_o^2A\nabla^2\chi_i\!\downarrow - f_o^2\chi_i\!\downarrow = \Phi_{e,had,ia}\!\downarrow + m_o^2AD_h\!\downarrow.$$

(A15)

Equation (A15) is a velocity potential form of the generalized ω equation for the balanced ageostrophic approximation in σ coordinates. In this equation the diabatic and advection terms computed by the ageostrophic wind are the same as those in the generalized ω equation in P coordinates [*Pauley and Nieman*, 1992], but the effect of orography on the vertical motion is better described. If equation (A15) is transformed into P coordinates, and the term $\Phi_{e,had,ia}\!\downarrow$ is computed by the geostrophic wind and expressed by $\Phi_{e,had,ia,g}\!\downarrow$, equation (A15) becomes a velocity potential form of the quasi-geostrophic ω equation. In order to reduce computational errors in the solution of (A15), a harmonic-sine spectral method [*Chen and Kuo*, 1992] is used.

From the solution χ_i of (A15), ω is calculated from (A8)

and $D = \nabla^2 \chi_l$. Using the continuity equation, the sigma vertical velocity is computed by

$$\dot{\sigma}_{k+\frac{1}{2}} = \sigma_{k+\frac{1}{2}} m^2 \sum_{j=1}^{N} D_j \Delta \sigma_j - m^2 \sum_{j=1}^{k} D_j \Delta \sigma_j$$

$$+ m^2 \sigma_{k+\frac{1}{2}} \sum_{j=1}^{N} \left(U_j \frac{\partial \ln p_*}{\partial x} + V_j \frac{\partial \ln p_*}{\partial y} \right) \Delta \sigma_j$$

$$- m^2 \sum_{j=1}^{k} \left(U_j \frac{\partial \ln p_*}{\partial x} + V_j \frac{\partial \ln p_*}{\partial y} \right) \Delta \sigma_j.$$

(A16)

The procedure for computing precipitation from the vertical motion is presented by *Chen et al.* [1997a]. Only large scale condensation is considered, and the computation procedure is similar to that discussed by *Arakawa and Lamb* [1977]. The temperature variation for a time step is computed from horizontal and vertical advection and adiabatic variation based on the thermodynamic equation. The specific humidity variation for a time step is deduced from the continuity equation for specific humidity. In these equations, the sigma vertical velocity, $\sigma_{k+1/2}$ is obtained from (A16). The precipitation rate is only computed for one time step, which is 30 mins, and then it is applied to a 12 hour period. The precipitation is calculated twice per day based on the operational analyses at 0000 and 1200 UTC from ECMWF. The annual precipitation is derived by adding daily precipitation amounts for the whole year.

References

Angell, J. K., Comparisons of variations in atmospheric quantities with sea surface temperature variations in the equatorial eastern Pacific, *Mon. Weather Rev.*, *109*, 230-243, 1981.

Appenzeller, C., J Schwander, S. Sommer, and T. F. Stocker, The NorthAtlantic Oscillation and its imprint on precipitation and ice accumulation in Greenland, *Geophys. Res. Lett.*, *25*, 1939-1942, 1998a.

Appenzeller, C., T. F. Stocker, and M. Anklin, North Atlantic Oscillation recorded in Greenland ice cores, *Science*, *282*, 446-449, 1998b.

Arakawa, A., and V. R. Lamb, Computational design of the basic dynamical process of the UCLA general circulation model, *Methods Comput Phys.*, *17*, 173-265, 1977.

Barlow, L. K., J. W. C. White, R. G. Barry, J. C. Rogers, and P. M. Grootes, The North Atlantic Oscillation signature in deuterium and deuterium excess signals in the Greenland Ice Sheet, *Geophys Res Lett.*, *20*, 2901-2904, 1993.

Barlow, L. K., J. C. Rogers, M. C. Serreze, and R. G. Barry, Aspects of climate variability in the North Atlantic sector: Discussion and relation to the Greenland Ice Sheet Project 2 high resolution isotopic signal, *J Geophys. Res.*, *102*(C12), 26,333-26,344, 1997.

Berthelsen, C., I. H. Mortensen, and E. Mortensen, Kalaallit Nunaat (Greenland Atlas), 127 pp., Greenl. Home Rule Gov., Nuuk, 1993.

Bromwich, D. H., and F. M. Robasky, Recent precipitation variations over the polar ice sheets, *Meteorol. Atmos. Phys.*, *51*, 259-274, 1993.

Bromwich, D. H., F. M. Robasky, R. A. Keen, and J. F. Bolzan,

Modeled variations of precipitation over the Greenland Ice Sheet, *J. Clim.*, *6*, 1253-1268, 1993.

Bromwich, D. H., R. I. Cullather, Q.-S. Chen, and B. M. Csatho, Evaluation of recent precipitation studies for the Greenland ice sheet, *J Geophys. Res.*, *103*(D20), 26,007-26,024, 1998.

Chapman, W. L., and J. E. Walsh, Recent variations of sea ice and air temperatures in high latitudes, *Bull. Am. Meteorol. Soc.*, *74*, 33-47, 1993.

Chen, Q.-S., and D. H. Bromwich, An equivalent isobaric geopotential height and its application to synoptic analysis and to a generalized ω equation in σ coordinates, *Mon. Weather Rev.*, *127*, 145-172, 1999.

Chen, Q.-S., and Y.-H. Kuo, A harmonic-sine series expansion and its application to the partitioning and reconstruction problem in a limited area, *Mon. Weather Rev.*, *120*, 91-112, 1992.

Chen, Q.-S., Y.-H. Kuo, and D. H. Bromwich, A balanced ageostrophic initialization with a fixed external wind lateral boundary value for limited-area models, *J. Meteorol. Soc. Jpn.*, *74*, 325-342, 1996.

Chen, Q.-S., D. H. Bromwich, and L. Bai, Precipitation over Greenland retrieved by a dynamic method and its relation to cyclonic activity, *J. Clim.*, *10*, 839-870, 1997a.

Chen, Q.-S., L. Bai, and D. H. Bromwich, A harmonic-Fourier spectral limited-area model with an external wind lateral boundary condition, *Mon. Weather Rev.*, *125*, 143-167, 1997b.

Gibson J. K., A. Hernandez, P. Kallberg, A. Nomura, E. Serrano, and S. Uppala, Current status of the ECMWF Re-Analysis Project, in *7th Symposium on Global Change Studies*, pp. 112-115, Am. Meteorol. Soc., Boston, Mass, 1996.

Haan, C. T., *Statistical Methods in Hydrology*, 378 pp., Iowa State Univ. Press, Ames, 1977.

Hurrell, J. W., Decadal trends in the North Atlantic Oscillation: Regional temperatures and precipitation, *Science*, *269*, 676-679, 1995.

Hurrell, J. W., and H. van Loon, Decadal variations in climate associated with the North Atlantic Oscillation, *Clim. Change*, *36*, 301-326, 1997.

Kalnay, E., et al., The NCEP/NCAR 40-year reanalysis project, *Bull. Am Meteorol. Soc.*, *77*, 437-471, 1996.

Meehl, G. A., and H. Van Loon, The seasaw in winter temperatures between Greenland and northern Europe, Part III, Teleconnections with lower latitudes, *Mon. Weather Rev.*, *107*, 1095-1106, 1979.

Ohmura, A., and N. Reeh, New precipitation and accumulation maps for Greenland, *J. Glaciol.*, *37*, 140-148, 1991.

Ohmura, A., M. Wild, and L. Bengtsson, A possible change in Greenland and Antarctic ice sheets in the coming century, *J. Clim.*, *9*, 2124-2135, 1996.

Ohmura, A., P. Calanca, M. Wild, and M. Anklin, Precipitation, accumulation and mass balance of Greenland Ice Sheet, *Z. Gletscherkd Glazialgeol.*, in press, 1999.

Pauley, P. M., and S. J. Nieman, A comparison of quasi-geostrophic and nonquasi-geostrophic vertical motions for a rapidly intensifying marine extratropical cyclone, *Mon. Weather Rev.*, *120*, 1108-1134, 1992.

Rogers, J. C., The association between the North Atlantic Oscillation and the Southern Oscillation in the Northern Hemisphere, *Mon. Weather Rev.*, *112*, 1999-2015, 1984.

Rogers, J. C., and H. van Loon, The seasaw in winter temperatures between Greenland and northern Europe, Part II, Some oceanic and atmospheric effects in middle and high latitudes, *Mon. Weather Rev.*, *107*, 509-519, 1979.

Rogers, J. C., J. F. Bolzan, and V. A. Pohjola, Atmospheric circulation variability associated with shallow-core seasonal isotopic extremes near Summit, Greenland, *J. Geophys. Res.*, *103*, 11,205-11,219, 1998.

Serreze, M. C., F. Carse, R. G. Barry, and J. C. Rogers, Icelandic low cyclonic activity: Climatological features, linkages with the NAO, and relationships with recent changes in the Northern Hemisphere circulation, *J. Clim.*, *10*, 453-464, 1997.

van Loon, H., and J. C. Rogers, The seasaw in winter temperatures

between Greenland and northern Europe, Part I, General description, *Mon. Weather Rev.*, *106*, 296-310, 1978.

White, J. W. C., L. K. Barlow, D. Fisher, P. Grootes, J. Jouzel, S. J. Johnsen, M. Stuiver, and H Clausen, The climate signal in the stable isotopes from Summit, Greenland: Results of comparisons with modern climate observations, *J. Geophys. Res.*, *102*, 26,425-26,439, 1997.

Yang, D., S. Ishida, B. E. Goodison, and T. Gunther, Bias correction of daily precipitation measurements for Greenland, *J. Geophys. Res.*, *104*, 6171-6181, 1999.

D.H. Bromwich, Q.-S. Chen, and Y.Li, Byrd Polar Research Center, Ohio State University, 1090 Carmack Road, Columbus, OH 43210-1002. (bromwich@polarmet1.mps.ohio-state.edu)

R.I. Cullather, Department of Aerospace Engineering Sciences, University of Colorado, Boulder, CO 80302.